Eur. Phys. J. B **50**, 587–592 (2006)
DOI: 10.1140/epjb/e2006-00178-9

THE EUROPEAN PHYSICAL JOURNAL B

Intrinsic tunnelling effects in self-doped $La_{0.89}MnO_3$ single crystals

V. Markovich[1], G. Jung[1,a], M. Belogolovskii[2], Y. Yuzhelevski[1], G. Gorodetsky[1], and Ya.M. Mukovskii[3]

[1] Department of Physics, Ben Gurion University of the Negev, P.O. Box 653, 84105 Beer Sheva, Israel
[2] Donetsk Physical and Technical Institute, National Academy of Sciences of Ukraine, 83114, Donetsk, Ukraine
[3] Moscow State Steel and Alloys Institute, 119991, Moscow, Russia

Received 23 November 2005 / Received in final form 20 February 2006
Published online 17 May 2006 –

Abstract. Transport properties of self-doped $La_{0.89}MnO_3$ single crystals with Néel temperature of $T_N \approx 139$ K have been investigated in wide temperature range 10–300 K. Data suggests that current at low temperature is conducted through a strongly temperature-dependent, but almost bias independent channel operating in parallel with a bias controlled but temperature independent channel. The first channel is associated with transport across an insulating antiferromagnetic matrix while the latter one represents tunnel conductivity through intrinsic tunnel junctions appearing due to interruption of conducting percolating paths by phase separated insulating inclusions. Tunnel character of the conductivity manifests itself in nonlinear current-voltage characteristics and appearance of a zero-bias anomaly in the form of a prominent conductance peak in the vicinity of zero bias. Zero bias anomaly and V-shaped characteristics of the differential conductance at high voltages are ascribed to the formation of local magnetic states in the insulating region of the tunneling junction.

PACS. 75.47.Gk Colossal magnetoresistance – 73.40.Gk Tunneling – 75.47.Lx Manganites

1 Introduction

Tunnel conductivity in manganite systems can be observed not only in artificial tunnel junctions fabricated by growing a barrier between manganate electrodes but also in spontaneous intrinsic tunnel junctions within the bulk of the material. The most investigated intrinsic junctions appear in layered manganites. For example, in widely investigated $(La,Sr)_3Mn_2O_7$ system, MnO_2 bi-layers are separated by layers containing La and Sr ions. With decreasing temperature the MnO_2 layers undergo a metal-insulator transition while the material sandwiched between them remains insulating [1]. Therefore, transport current directed perpendicular to the layers is flowing by means of sequential spin polarized tunneling through intrinsic tunnel barriers between adjacent layers [2]. Spontaneous tunnel barriers are also formed on surfaces of manganite single crystals and epitaxial films due to existence of dead layers formed by the outermost MnO_2 bi-layers. The surface magnetic state of manganites differs from the bulk one due to reduced magnetic coupling, chemically different composition of the surface layer, or oxygen deficiency. As a result the surface sheet of a layered manganite is depleted from charge carriers, looses long-range ferromagnetic (FM) order and acts as an intrinsic tunnel barrier [3–6].

Another type of intrinsic tunnel barriers associated with extended crystalline defects such as grain or twin boundaries appears in the bulk of manganite crystals and films. Creation of an insulating region near an extended defect is attributed to bond angle variations disturbing the double exchange mechanism [7], electronic band bending effects due to strain fields associated with such defects [8], or to phase separation at internal interfaces [9,10]. Grain boundary type intrinsic tunnel junctions are prone to dominate in polycrystalline manganites while in good quality single crystals defects associated with twin boundaries are more pronounced. Manganite single crystals are twinned in a structural transition occurring when crystals are cooled down to room temperatures after the crystallization process [11]. Magneto-optics investigations revealed that in low hole-doped $La_{1-x}Ca_xMnO_3$ (LCMO) single crystals twin domains pin FM domain walls and enhance the strength of intrinsic tunnel effects [12]. In low-doped LCMO crystals twin and domain boundary tunnel junctions operate together with junctions appearing as a result of pronounced intrinsic phase separation. In phase separated manganites tunnel barriers may be formed when a percolating metallic path is interrupted by insulating inclusions of the less conducting phase [13].

[a] e-mail: jung@bgumail.bgu.ac.il

Transport measurements, completed by magneto-optic investigations, suggested that low temperature resistivity of the underdoped LCMO compounds is dominated by tunneling across intrinsic barriers associated with twin domains, while phase separation dominates in compounds doped close to the critical doping level $x_C = 0.225$, which separates nominally ferromagnetic insulating ground state from a ground state with a FM metallic character [12].

It has to be underlined that in a difference to fabricated discrete tunnel junctions, one cannot provide an absolute direct proof of the tunnel character of the conductivity when it is dominated by intrinsic tunnel junctions. In this case only an indirect evidence can be brought from observations of nonlinear voltage-current ($V - I$) characteristics and their temperature evolution, provided both can be well fitted to a tunneling model. In recent investigations of metastable nonlinear resistivity in $x = 0.18$ LCMO crystal we have reproduced experimentally observed $V - I$ characteristics and the temperature dependence of the resistivity $R(T)$ using a model incorporating hopping, metallic, and tunnel conductivity channels, dominating at high, intermediate, and low temperatures, respectively. At low temperatures the voltage dependence of the dynamic resistance $R_d(V)$ was well fitted to the direct tunnel conductivity model [14], or with even better accuracy, to the Glasman and Matveev model [15] of indirect tunneling [13]. In this paper we show that intrinsic tunnel junctions dominate low temperature transport properties not only of low hole-doped manganites but also those of so-called self-doped $La_{1-x}MnO_3$ crystals. The parent $LaMnO_3$ compound is known to be an A-type AFM insulator with the Néel temperature $T_N \approx 139$ K [16]. At room temperature it has an orthorhombic perovskite structure with the space group *Pnma* and shows antiferrodistorsive orbital ordering of Mn-O bond configurations [17].

Self-doped $LaMnO_3$ (LMO) crystals are known to be phase separated into metallic FM clusters dispersed in an antiferromagnetic (AFM) insulating matrix. The formulae frequently used for the off-stoichiometric compound is $LaMnO_{3+\delta}$. However, the perovskite structure cannot accommodate the excess of oxygen in interstitial sites that leads to appearance of cationic vacancies [18,19]. Therefore, the actual chemical formulae should be rather written as $La_{1-x}Mn_{1-y}O_3$.

Our research was motivated by our previous studies of the transport properties of low doped LCMO crystals and by recent investigations of self-doped $La_{1-x}MnO_3$ crystals in which an evidence for the presence of FM clusters, even in the paramagnetic phase well above the Néel temperature, was found in transport, magnetic and magnetic resonance data [20].

2 Experimental and results

$La_{0.89}MnO_3$ single crystals were grown by a floating zone method using radiative heating. The composition of our samples was verified by inductively coupled plasma-atomic emission spectroscopy. We have found that the chemical composition of the crystals corresponds to the nominal composition of starting materials with the ratio of La and Mn ions of 0.89:1 ± 0.01 leading us to the conclusion that in our samples $y = 0$. The X-ray data of the crystals were compatible with an orthorhombic unit cell of the space group *Pnma* ($a = 5.7265$ Å, $b = 7.7003$ Å, $c = 5.533$ Å) of a perovskite structure.

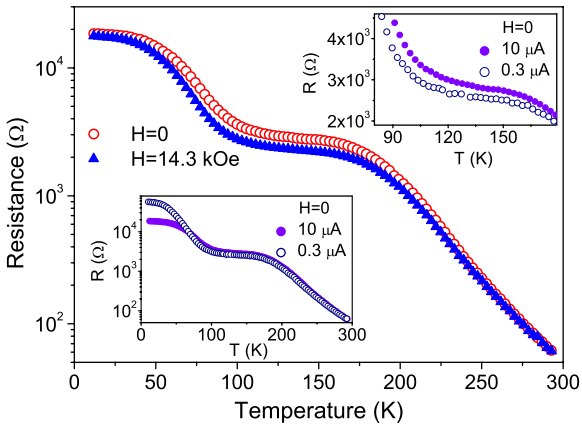

Fig. 1. The resistivity of $La_{0.89}MnO_3$ single crystal as a function of temperature at zero magnetic field and at $H = 14.3$ kOe as recorded in the heating run with dc current bias of 10 μA. The insets show bias current influence on the $\rho(T)$ dependence: full symbols: 10 μA, open symbols 0.3 μA. Lower inset — logarithmic scale, entire temperature range, upper inset — linear scale restricted, enlarged temperature range.

For transport measurements sample of $7 \times 4 \times 1.5$ mm^3, with the longest dimension along ⟨110⟩ direction, was cut out of the as grown crystal. The electrodes for conventional four-point measurements were made by vacuum evaporating gold strips on the crystal surface. The distance between the voltage contacts was 300 μm. Resistivity as a function of temperature and magnetic field was measured directly by using dc current bias, or alternatively, ac bias and a standard lock-in technique. In order to prevent spurious heating effects during the resistivity measurements, dc bias current was restricted to a sufficiently small level within 0.3–10 μA range. In the differential resistance dV/dI and differential conductance dI/dV measurements we have employed ∼0.5 μA ac current at 426 Hz. Magnetoresistance (MR) measurements were carried out at magnetic fields H up to 15 kOe, applied parallel to the current direction. Cylinder-shaped samples with diameter of 1 mm and height of about 4 mm along ⟨110⟩ axis were prepared for magnetic measurements performed using vibrating sample magnetometer [20].

Figure 1 shows the temperature dependence of the resistivity $\rho(T)$ of a $La_{0.89}MnO_3$ single crystal recorded during slow cooling of the sample biased with 10 μA dc current flow in magnetic field $H = 0$ (ZFC) and $H = 14.3$ kOe (FC). We have found that the resistivity measured during the subsequent heating run practically coincides with that recorded during the cooling cycle.

For temperatures above $T \approx 235$ K the ZFC $\rho(T)$ dependence can be well fitted to a simple Arrhenius law $\rho(T) = \rho_0 \exp(E_a/kT)$ with a single activation energy

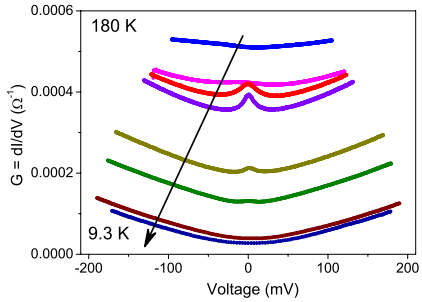

Fig. 2. The dynamic conductance dI/dV of $La_{0.89}MnO_3$ single crystal versus bias voltage at 180 K, 160 K, 140 K, 120 K, 100 K, 80 K, 50 K, and 9.3 K. The arrow indicates the direction of decreasing temperature.

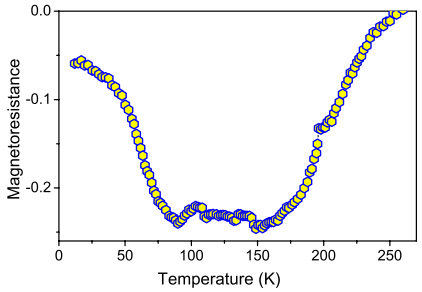

Fig. 3. Magnetoresistance $[R(14.3\ \text{kOe}) - R(0)]/R(14.3\ \text{kOe})$ as a function of temperature.

$E_a = 0.19$ eV. As a clear sign of changes in the conduction mechanism $\rho(T)$ starts to deviate from the exponential dependence at temperatures below $T \approx 235$ K. Between 170 K and 110 K the resistivity is almost temperature independent and starts to increase again only at lower temperatures, to reach yet another resistance plateau at $T \approx 50$ K. The insets to Figure 1 show the measuring current influence upon the sample resistance. At temperatures below ≈180 K the $V - I$ characteristics became nonlinear, however, their non-Ohmic character is most pronounced at temperatures below 50 K.

Voltage dependence of the differential conductance $G = dI/dV$ is illustrated in Figure 2. At high temperatures, where the $V - I$ curves are almost linear, the conductance depends very weakly on bias. With decreasing temperature a significant change in $G(V)$ occurs. The overall nonlinear shape of the $G(V)$ starts to resemble that of a tunnel junction. In the temperature range 80–160 K a strongly temperature dependent zero-bias anomaly appears in $G(V)$ characteristics. In a typical magnetic tunnel junction zero bias anomaly (ZBA) takes form of a sharp conductivity minimum [21–24]. In a marked difference, the ZBA observed in the self-doped $La_{0.89}MnO_3$ single crystal appears as a conductivity maximum at zero bias. For the magnetic fields accessible in our experiments, the ZBA is practically field independent.

The temperature dependence of magnetoresistance defined as $MR = [R(14.3\ \text{kOe}) – R(0)]/R(14.3\ \text{kOe})$ is shown in Figure 3. Unexpectedly, a significant negative magneresistance $MR \approx 24\%$ appears far above the Néel temperature determined from magnetic measurements,

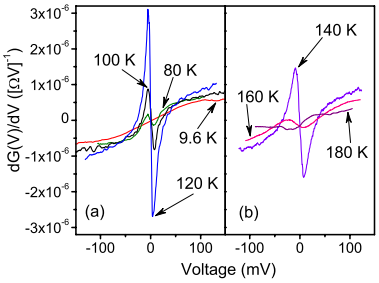

Fig. 4. The derivative of the sample conductance $dG(V)/dV = d^2I(V)/dV^2$ as a function of voltage: (a) in the temperature interval 9.6–120 K and (b) in the temperature range 140–180 K. Observe that ZBA appears at $T \approx 160$ K, initially increases with decreasing temperature, reaches a maximum at $T \approx 120$ K, and decreases with further temperature decrease, to disappear completely at $T < 80$ K.

$T_N = 139$ K. Since the resistance is measured at very low current the MR plateau observed in the temperature range 80–170 K results, among others, from the appearance of a pronounced zero-bias anomaly in the same temperature range.

3 Discussion

The analysis of experimental $G(V)$ characteristics shows that the temperature influence on the overall behavior of $G(V)$ can be reduced to a trivial voltage independent conductivity shift $\Delta G(T)$, gradually increasing with decreasing temperature. The significant temperature dependent effect is observed only at voltages $|V| < 50$ mV in a relatively narrow temperature range between 80 and 160 K as ZBA.

To demonstrate clearly the above claim, in Figure 4 we show the second derivative of the $I - V$ characteristics $d^2I(V)/dV^2 = dG(V)/dV$. Remarkably, one sees almost identical high-voltage behavior, beyond the ZBA range, for all temperatures up to 160 K. The identical voltage behavior of the second derivative clearly results from removal of the voltage-independent shift $\Delta G(T)$ in the differentiation process.

The results of our analysis lead us to a conclusion that self-doped manganites at low temperatures conduct current through two distinct channels. The conductivity of the first channel strongly depends on temperature but is not influenced by the bias while the second, temperature independent one, is strongly influenced by the voltage. In reality the current flows across an AFM insulating matrix containing FM conducting clusters. Properties of the first channel are determined by the temperature dependence of the bulk resistivity of an AFM matrix. The charge carriers in the second channel are transferred by means of tunneling through insulating regions interrupting the conducting percolation paths.

Within such a scenario for intrinsic tunnel junctions the height of the corresponding tunnel barrier can be estimated from the $LaMnO_3$ band structure. Theoretical calculations indicate that there is a direct energy gap of

the order of a fraction of an electronvolt in the insulating phase of $LaMnO_3$ [25]. Observe that this value is consistent with the activation energy $E_a = 0.19$ eV determined by us from $R(T)$ data above T_N.

For voltages at which the product eV is smaller than the tunneling barrier height, i.e., within the entire voltage range of our experiments, the contribution of elastic tunneling processes usually has a parabolic dependence on V [14,26]:

$$G_{el} = G_0 + \alpha V + \beta V^2. \quad (1)$$

On the background of the G_{el} a fine structure may appear due to inelastic scattering of charge carriers with bosonic near-interface excitations [26]. The intensity of the fine structure depends on the interactions strength:

$$G_{in} \propto \int_0^{e|V|} F(\omega) d\omega, \quad (2)$$

where $F(\omega)$ is the spectrum of excitations.

The $G(V)$ curves follow the behavior predicted for the tunneling channel by equation (1) in a wide temperature range. Indeed, with the exclusion of the ZBA contribution, the second derivative $d^2I(V)/dV^2$ in Figure 4 is a linear function of voltage in a wide temperature range. Only at high voltages and temperatures close to the nonlinearity onset, $T > 160$ K and at low temperatures, $T < 100$ K, the $d^2I(V)/dV^2$ curve deviates from linear behavior. This behavior, usually referred to as a V-shaped curve, was observed in point contact tunnel junctions between Ag tip and superconducting cuprate or manganite electrode [6]. The V-shaped $G(V)$ has been explained as a result of inelastic interactions with a broad continuum of bosonic excitations inside the barrier for which $F(\omega) = \text{const}$ in a wide energy range.

Yet another feature testifying about the possible tunnel character of the conductivity at low temperatures is the zero-bias anomaly. It was found that the ZBA is very sensitive to the material properties of the barrier. Different theoretical explanation of the ZBA were proposed. They include modified electron density of states due to the interference between the electron waves scattered by an impurity [27], scattering of hot electrons from the emitting electrode by localized magnetic moments at the interfaces between the magnetic electrodes and the barrier [22,23], and interactions of the tunneling electrons with magnons and phonons [24].

It was shown by Anderson [28], that an exchange interaction of an impurity with the nearby metal causes a logarithmic peak at the Fermi level that reveals itself in the tunneling conductance as a maximum centered at $V = 0$. The relating excess conductance, defined as a difference between the measured differential conductance and the background elastic-tunneling characteristic is described by [28,29]:

$$\Delta G(V) = G(V) - G_{el}(V) = N_e N_{imp} \ln\left[E_0/(e|V| + k_B T)\right]. \quad (3)$$

Here N_e is the density of states at the Fermi energy of the conducting electrode, N_{imp} is the density of localized magnetically uncorrelated spins, E_0 is a cutoff energy, an unknown parameter in the theory. The theory of magnetic tunnel junction predicts that ZBA conductance peak due to localized magnetic moments should logarithmically depend on voltage and temperature and have an amplitude of few percents of $G_{el}(V = 0)$ [29,30].

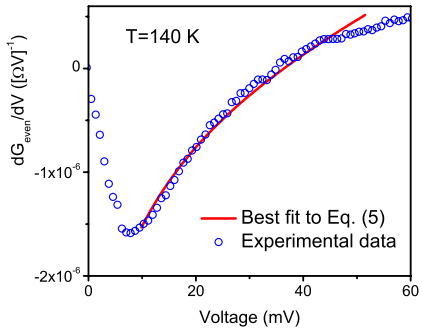

Fig. 5. The comparison of fitted and experimental dependencies of the voltage derivative of the conductivity dG/dV for $T = 140$ K.

To avoid the unknown parameter E_0 in the analysis we have calculated the even parts of the conductance curves

$$G_{even}(V) = \frac{G(+V) + G(-V)}{2} = G_0 + \beta V^2 + \Delta G(V), \quad (4)$$

differentiated them numerically, and compared with the relation

$$\frac{dG_{even}(V)}{dV} = aV + \frac{b}{e|V| + k_B T}, \quad (5)$$

where $a = 2\beta$ and b are the fitting parameters. We have found a reasonable agreement, as shown in Figure 5, of the experimental $dG(V)/dV$ curves with equation (5) in entire ZBA voltage range for temperatures between 100 and 140 K. We have found that the influence of the fitting parameter a is small and that this parameter only weakly depends on temperature.

Appelbaum argued that the relation (3) used by us is valid only for small voltages not exceeding $V^* \sim k_B T/e$ [29]. In accordance with the theoretical predictions we have observed a local minimum of $dG_{even}(V)/dV$ at a voltage almost coinciding with V^*.

Our results provide thus an indirect evidence for the existence of intrinsic tunnel junctions in self-doped manganite single crystals. The junctions seem to appear due to pronounced phase separation at low temperatures. In self-doped manganites La vacancies create domains of Mn^{4+} ions coupled to the surrounding Mn^{3+} ions by the ferromagnetic double exchange that results in appearance of short-ranged FM domains inside a paramagnetic matrix at $T > T_N$ and inside an AFM matrix at $T < T_N$. Electron magnetic resonance (EMR) studies have shown that magnetically ordered state of La-deficient samples is inhomogeneous, and composed of several FM phases immersed in an AFM matrix. For $La_{0.87}MnO_3$ crystal, having composition and magnetic characteristics which are very close to those of our samples [20], at least two signals from distinct FM phases were distinguished. Clear resonant absorption signals from distinct FM phases appear

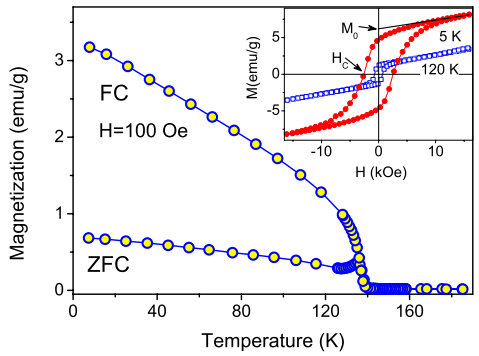

Fig. 6. Field cooled (M_{FC}) and zero field cooled magnetization (M_{ZFC}) of $La_{0.89}MnO_3$ crystal, measured at an applied magnetic field $H = 100$ Oe. Inset shows the hysteresis loop of $La_{0.89}MnO_3$ crystal at $T = 5$ K and $T = 120$ K. At $T > 140$ K the dependence is linear at all fields and no traces of spontaneous magnetization can be directly seen.

subsequently at $T = 235$ K and $T = 180$ K [20]. The reason for such a variety of FM phases can be attributed to strong inhomogeneity of the La vacancy distribution. Note that onset temperature of the FM signals coincides with the temperature where $R(T)$ dependence starts to depart from a simple Arrhenius law.

Measurements of the magnetization as a function of temperature and magnetic field applied along the direction the maximum magnetization in (110) plane have shown, see Figure 6, that the magnetization is very small at temperatures $T > 140$ K. With increasing temperature ZFC magnetization exhibits a sharp maximum at $T \approx 133$ K and drops to zero. The temperature of the abrupt change in the FC magnetization occurring during cooling at $T \approx 139$ K is identified with the antiferromagnetic transition temperature T_N by comparing temperature evolution of magnetization for pure $LaMnO_3$, for which the Neel temperature is well known, with that of several $La_{1-x}MnO_3$ crystals [20]. It turns out that in the above crystals the amount of the ferromagnetic phase increases with increasing x but the Neel temperature is practically doping independent [20].

A hysteresis loops for $La_{0.89}MnO_3$ crystal at $T = 5$ K and $T = 120$ K are shown in the inset to Figure 6. Weak ferromagnetic moment results likely from the presence of FM clusters. The value for the spontaneous magnetization $M_0 = 5.8$ emu/g at $T = 5$ K was evaluated from a linear extrapolation of the high field magnetization to zero field. The coercive field H_C is 2.8 kOe at $T = 5$ K. Confrontation of the magnetization data shown in Figure 6 with EMR results leads us to a conclusion that in the paramagnetic temperature range, $T > 140$ K both Mn^{3+} and of Mn^{3+}–Mn^{4+} subsystems practically do not interact leading to very small magnetization [20]. This is also consistent with the observation that small short-range FM clusters start to exist at $T > 200$ K while the long-range magnetic order appears only below $T_N = 139$ K.

The appearance of intrinsic tunnel junctions in the bulk of the material requires that insulating regions be necessarily only few nanometer thick. This seems to be inconsistent with the observed low level of magnetization at low temperatures. The apparent controversy is removed if one assumes that conducting FM paths are filamentary. The existence of filamentary structures in several phase separated manganite compounds has been experimentally confirmed by low angle neutron scattering spectroscopy [32].

The temperature evolution of the ZBA, which is most pronounced in the range 100–140 K and completely disappears at $T < 80$ K is a new feature that to our best knowledge has not been observed before. It contradicts all existing ZBA models and can only be accommodated with the Appelbaum-Andreson theory. In alternative models based on indirect tunneling through localized states [33,34], the differential conductance peaks at the voltage corresponding to the energy in the center of the localized states band. This energy is anywhere in the middle of the gap and does not coincide with the Fermi level. Therefore, the resulting ZBA peak should be asymmetric with respect to the bias (shifted from the zero voltage. The ZBA observed in our experiments is almost symmetric. The height of the peak predicted by the alternative models increases with decreasing temperature. This contradicts the experimental behavior of the ZBA peak disappearing at low temperatures. This behavior can only be accommodated within the Appelbaum-Andreson theory by assuming that the origin of the ZBA is related to the interaction of charge carriers with magnetic moments appearing in a restricted temperature range inside the barrier. Finally, according to the alternative models the conductivity in the peak range scales as $1/V^2$, whereas the experimental data fit well the logarithmic dependence predicted by the Appelbaum-Anderson model.

ZBA may be therefore attributed to the development of various FM phases which act as conducting banks for intrinsic tunnel junctions and to the competition between the parallel conductivity channels. If the ZBA is related to the scattering on the local magnetic moments from FM phases then this process will be sensitive to the temperature evolution of the magnetic anisotropy and spontaneous magnetization of coexisting FM phases. The amplitude of ZBA increases with decreasing temperature following the increase of the spontaneous magnetization. However, when thermal fluctuations term k_BT in equation (3) becomes comparable to the interaction energy, then the density of free spins N_{imp} decreases, more scattering centers become inactive and do not take part in the tunneling processes. Consequently, the zero-bias conductance peak goes through a maximum around $T = 120$ K and decreases with further temperature decrease.

In conclusion, the nonlinear character of $V - I$ curves and the appearance of zero-bias anomaly provide an indirect experimental evidence for the presence of intrinsic tunnel junctions in self-doped manganite single crystals. Analysis of the experimental data suggests that intrinsic tunnel barriers are formed due to pronounced phase separation into conducting ferromagnetic clusters immersed in an insulating antiferromagnetic matrix at low temperature. Pronounced zero-bias anomaly, which appears in

the form of a conductivity peak, seems to be related to the presence of uncorrelated magnetic moments at the barrier/electrode interface. The same mechanism is proposed to explain V-like behavior of the conductivity vs. bias characteristics at high voltages.

Transport properties of self-doped $La_{0.89}MnO_3$ crystals are partly similar to those of hole doped $La_{0.82}Ca_{0.18}MnO_3$, $La_{0.78}Ca_{0.22}MnO_3$, and $Pr_{0.78}Sr_{0.22}MnO_3$ single crystals, previously investigated by us [12,14,31]. One should note however, that the origin of the intrinsic tunnel junctions and the nature of ZBA in the hole-doped manganites might be different from those reported in the present work. For example, in $La_{0.82}Ca_{0.18}MnO_3$ crystals we have observed ZBA both in the form of conductivity maximum, as in this work, and as a conductivity minimum, which is typical for magnetic tunneling junctions [31]. Therefore, a comprehensive understanding of low temperature transport properties of manganites and in particular the nature and physics of intrinsic tunnel junctions still requires more dedicated theoretical and experimental studies.

This research was supported by the Israeli Science Foundation administered by the Israel Academy of Sciences and Humanities (grant 209/01). The assistance offered by Dr. D. Mogilyansky in X-ray measurements and by Dr. I. Fita in magnetic measurements is greatly acknowledged. Ya. M.M. acknowledges the support obtained from ISTC grant 1859.

References

1. S. Heim, T. Nachtrab, M. Mösle, R. Kleiner, R. Koch, S. Rother, O. Waldmann, P. Müller, T. Kimura, Y. Tokura, Physica C **367**, 348 (2002)
2. J.W. Freeland, K.E. Gray, L. Ozyuzer, P. Berghuis, E. Badica, J. Kavich, H. Zheng, J.F. Mitchell, Nature Materials **4**, 62 (2005)
3. J.Z. Sun, D.W. Abraham, R.A. Rao, C.B. Eom, Appl. Phys. Lett. **74**, 3017 (1999)
4. J. O'Donnel, A.E. Andrus, S. Oh, E.V. Colla, J.N. Eckstein, Appl. Phys. Lett. **76**, 1914 (2000)
5. J.H. Park, E. Vescovo, H.J. Kim, C. Kwon, R. Ramesh, T. Venkatesan, Phys. Rev. Lett. **81**, 1953 (1998); J.H. Park, E. Vescovo, H.J. Kim, C. Kwon, R. Ramesh, T. Venkatesan, Nature **392**, 794 (1998)
6. M.A. Belogolovskii, Yu. F. Revenko, A. Yu. Gerasimenko, V.M. Svistunov, E. Hatta, G. Plitnik, V.E. Shaternik, E.M. Rudenko, Low Temp. Phys. **28**, 391 (2002) [Fiz. Nizk. Temp. **28**, 553 (2002)]
7. J.E. Evetts, M.G. Blamire, N.D. Mathur, S.P. Isaac, B.-S. Teo, L.F. Cohen, J.L. MacManus-Driscoll, Philos. Trans. R. Soc. London, Ser. A **356**, 1593 (1998)
8. R. Gross, L. Alff, B. Buechner, B.H. Freitag, C. Hoefener, J. Klein, Y. Lu, W. Mader, J.B. Philipp, M.S.R. Rao, P. Reutler, S. Ritter, S. Thienhaus, S. Uhlenbruck, B. Wiedenhorst, J. Magn. Magn. Mater. **211**, 150 (2000)
9. M.-H. Jo, N.D. Mathur, N.K. Todd, M.G. Blamire, Phys. Rev. B **61**, R14905 (2000)
10. M. Bibes, L. Balcells, J. Fontcuberta, M. Wojcik, S. Nadolski, E. Jedryka, Appl. Phys. Lett. **82**, 928 (2003)
11. B.B. Van Aken, A. Meetsma, Y. Tomioka, Y. Tokura, T.T.M. Palstra, Phys. Rev. B **66**, 224414 (2002); B.B. Van Aken, Ph. D. Thesis, University of Groningen (2001), `www.ub.rug.nl/eldoc/dis/science.`
12. V. Markovich, Y. Yuzhelevski, G. Gorodetsky, G. Jung, C.J. van der Beek, Ya.M. Mukovskii, Europ. Phys. J. B **35**, 295 (2003)
13. V. Markovich, G. Jung, Y. Yuzhelevski, G. Gorodetsky, A. Szewczyk, M. Gutowska, D.A. Shulyatev, Ya.M. Mukovskii, Phys. Rev. B **70**, 064414 (2004); Y. Yuzhelevski, V. Markovich, V. Dikovsky, E. Rozenberg, G. Gorodetsky, G. Jung, D.A. Shulyatev, Ya.M. Mukovskii, Phys. Rev. B **64**, 224428 (2001); G. Jung, V. Markovich, Y. Yuzhelevskii, E. Rozenberg, G. Gorodetsky, Ya.M. Mukovskii, J. Appl. Phys. **97**, 10H708 (2005)
14. J.G. Simmons, J. Phys. D **4**, 613 (1971)
15. L.I. Glasman, K.A. Matveev, Sov. Phys. JETP **67**, 1276 (1988)
16. J.B. Goodenough, "Rare Earth-Manganese Perovskites", *Handbook on the Physics and Chemistry of Rare Earth*, Vol. 33, edited by K.A. Gschneidner Jr., J.-C.G. Bunzli, V. Pecharsky (Elsevier Science, 2003)
17. J. Rodriguez-Carvajal, M. Hennion, F. Moussa, A.H. Moudden, L. Pinsard, A. Revcolevschi, Phys. Rev. B **57**, R3189 (1998)
18. J.A.M. van Roosmalen, E.H.P. Cordfunke, R.B. Helmholdt, H.W. Zandbergen, J. Solid State Chem. **110**, 100 (1994); J.A.M. van Roosmalen, E.H.P. Cordfunke, *ibid.* **110**, 106 (1994)
19. J. Topfer, J.B. Goodenough, J. Solid State Chem. **130**, 117 (1997); J. Topfer, J.B. Goodenough, Chem. Mater. **9**, 1467 (1997)
20. V. Markovich, I. Fita, A.I. Shames, R. Puzniak, E. Rozenberg, Ya. Yuzhelevski, D. Mogilyansky, A. Wisniewski, Ya.M. Mukovskii, G. Gorodetsky, J. Phys. Condens. Matter. **15**, 3985 (2003)
21. S. Mukhopadhyay, I. Das, S.P. Pai, P. Raychaudhuri, Appl. Phys. Lett. **86**, 152108 (2005)
22. S. Zhang, P.M. Levy, A.C. Marley, S.S.P. Parkin, Phys. Rev. Lett. **79**, 3744 (1997)
23. L. Sheng, D.Y. Xing, D.N. Sheng, Phys. Rev. B **70**, 094416 (2004)
24. J.S. Moodera, J. Nowak, R.J.M. van de Veerdonk, Phys. Rev. Lett. **80**, 2941 (1998)
25. W.E. Pickett, D.J. Singh, Phys. Rev. B **53**, 1146 (1996)
26. E.L. Wolf, *Principles of Electron Tunneling Spectroscopy* (Oxford University Press, New York, 1989)
27. A.M. Rudin, I.L. Aleiner, L.I. Glazman, Phys. Rev. B **55**, 9322 (1997)
28. P.W. Anderson, Phys. Rev. Lett. **17**, 95 (1966)
29. J.A. Appelbaum, Phys. Rev. **154**, 633 (1967)
30. R.H. Wallis, A.F.G. Wyatt, Phys. Rev. Lett. **29**, 479 (1972)
31. V. Markovich, E. Rozenberg, Y. Yuzhelevski, G. Jung, G. Gorodetsky, D.A. Shulyatev, Ya.M. Mukovskii, Appl. Phys. Lett. **78**, 3499 (2001)
32. M. Viret, F. Ott, J.P. Renard, H. Glättli, L. Pinsard-Gaudart, A. Revcolevschi, Phys. Rev. Lett. **93**, 217402 (2004)
33. E.Y. Tsymbal, A. Sokolov, I.F. Sabirianov, B. Doudin, Phys. Rev. Lett. **90**, 186602 (2003)
34. V. Garcia, H. Jaffrès, M. Eddrief, M. Marangolo, V.H. Etgens, J.-M. George, Phys. Rev. B **72**, 081303 (2005)